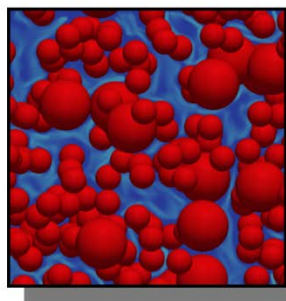
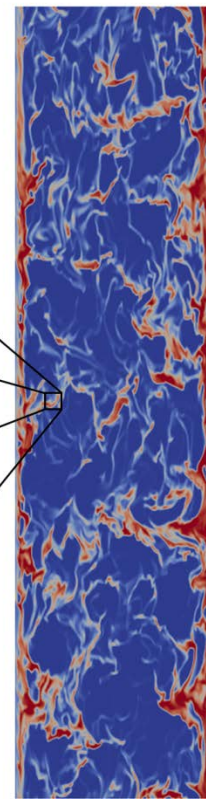
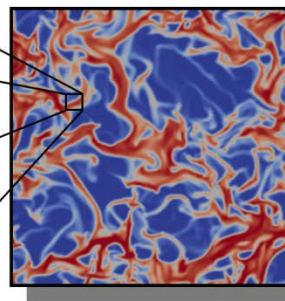


## MFiX Simulations

**MFiX** DEM



**MFiX** TFM



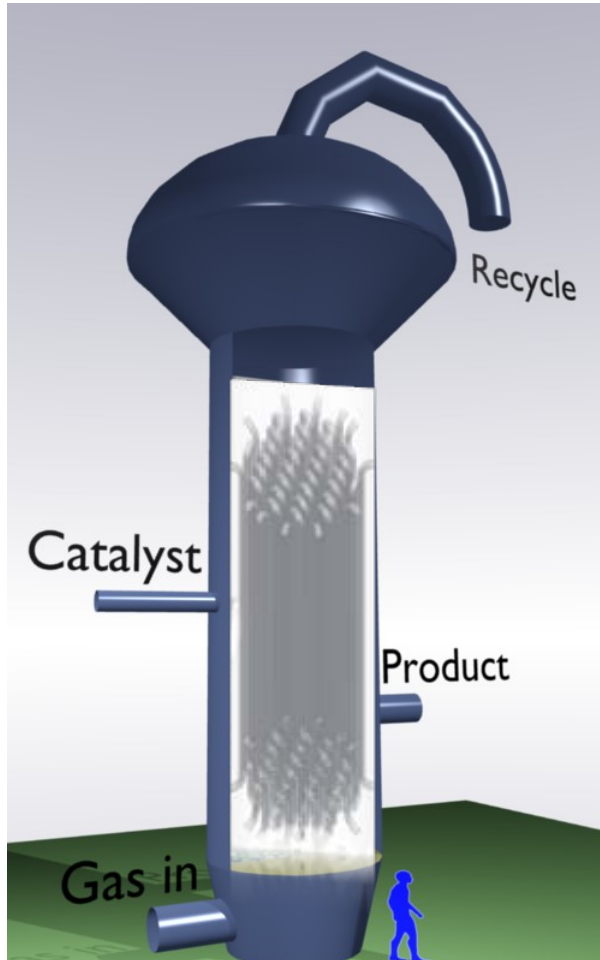
Hydrodynamics of gas-solids flow in a bubbling fluidized bed with immersed vertical U-tube banks

Vikrant Verma

Tingwen Li, Jean-François Dietiker,  
William A. Rogers

12<sup>th</sup> August, 2015

- **Fluidization**
- **Motivation**
- **Two fluid model**
- **Cut-cell method**
- **Geometry configuration**
- **Post processing**
- **Simulations results**
  - Bubble properties
  - Solids motion
- **Conclusions**



**Gas-solid contacting** in many different processes:

- polymerization
- fluid-catalytic cracking
- dry roasting
- Combustion and gasification
- ...

**Reactors:**

**Fluidized bed** (fluidization: drag equals weight)

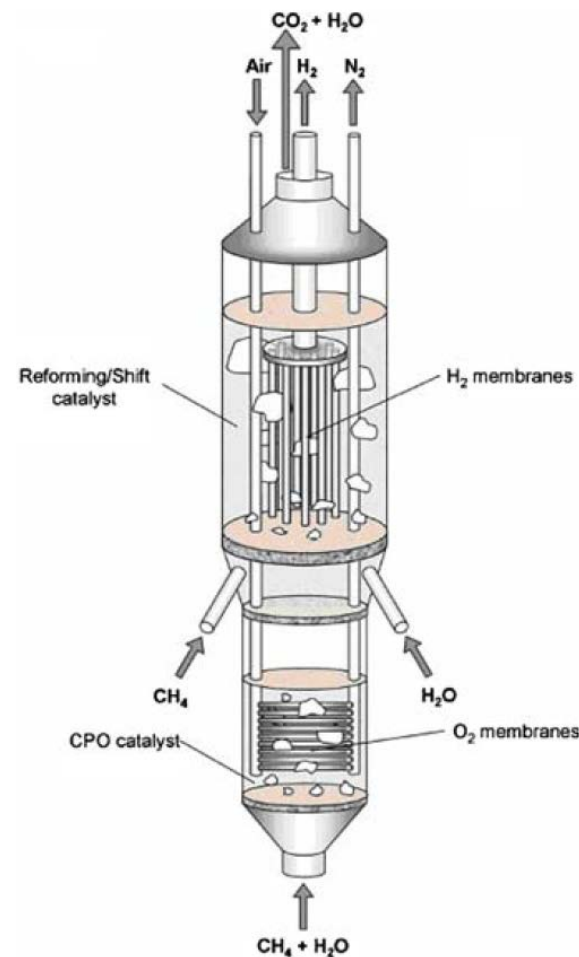
**Key characteristics: intrinsically multiscale**

- p-p & p-g interactions at  $1-5 d_p$
- flow structures ( $10-100 d_p$ )
- gas-solid behavior (industrial size: many other factor)

# Motivation



- ❑ In industrial fluidized-bed applications, internals such as heat exchanger tubes and baffles are regularly employed
- ❑ Immersed internals modify the gas–solid flow structure and thus may have significant effects on the fluidization
- ❑ Complex hydrodynamics in bubbling fluidized beds with immersed internals are still difficult to describe.
- ❑ The effectiveness of internals is greatly dependent on their design (horizontal/vertical tubes, packing, baffles...)
- ❑ Experimental study of FBs with internals is challenging
- ❑ CFD has an advantage to investigate this complex hydrodynamics
- ❑ **Supporting CFD study of 1 MW pilot plant at ADA-Inc under CCSI, where internal vertical tubes in the FB acts as a heat exchangers.**



- **Generalized Navier-Stokes equations for interacting continua**

Mass conservation equations

$$\frac{\partial(\varepsilon_g \rho_g)}{\partial t} + \nabla \cdot (\varepsilon_g \rho_g \bar{u}_g) = 0 \qquad \frac{\partial(\varepsilon_s \rho_s)}{\partial t} + \nabla \cdot (\varepsilon_s \rho_s \bar{u}_s) = 0$$

Momentum conservation equations

$$\frac{\partial(\varepsilon_g \rho_g \bar{u}_g)}{\partial t} + \nabla \cdot (\varepsilon_g \rho_g \bar{u}_g \bar{u}_g) = -\varepsilon_g \nabla p_g - \nabla \cdot (\varepsilon_g \bar{\tau}_g) - \beta(\bar{u}_g - \bar{u}_s) + \varepsilon_g \rho_g \bar{g}$$

$$\frac{\partial(\varepsilon_s \rho_s \bar{u}_s)}{\partial t} + \nabla \cdot (\varepsilon_s \rho_s \bar{u}_s \bar{u}_s) = -\varepsilon_s \nabla p_g - \nabla p_s - \nabla \cdot (\varepsilon_s \bar{\tau}_s) + \beta(\bar{u}_g - \bar{u}_s) + \varepsilon_s \rho_s \bar{g}$$

Granular temperature balances

$$\frac{3}{2} \left[ \frac{\partial}{\partial t} (\varepsilon_s \rho_s \Theta) + \nabla \cdot (\varepsilon_s \rho_s \Theta \bar{u}_s) \right] = - (p_s \bar{I} + \varepsilon_s \bar{\tau}_s) : \nabla \bar{u}_s - \nabla \cdot (\varepsilon_s q_s) - 3\beta\Theta - \gamma$$

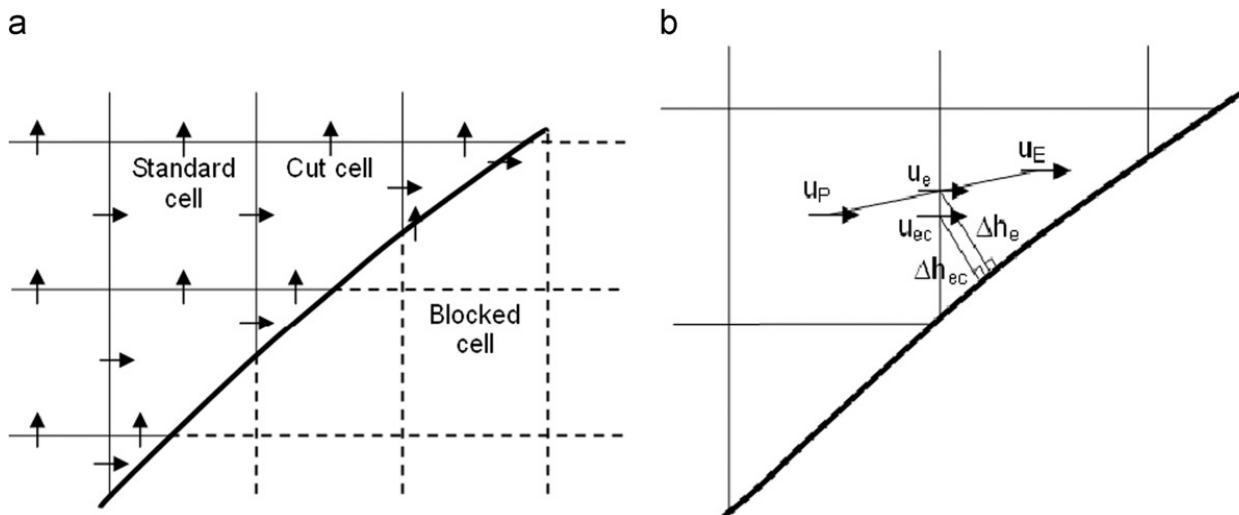
# Cut cell method for internal surface



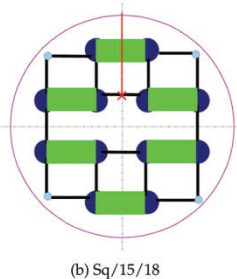
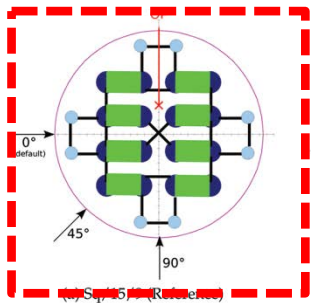
The internal surface (thick solid line) partition computational domain into three types of cells :

- (1) standard (uncut) cells;
- (2) cut-cells that require special treatment to incorporate the presence of the solid wall/surface (velocity nodes are adjusted to the center of the cut cell)
- (3) blocked cells that are excluded from computations since they are located outside the active computational domain.

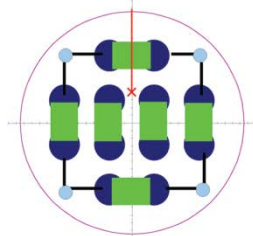
A no-slip or free-slip velocity boundary condition can be applied for each phase at the wall.



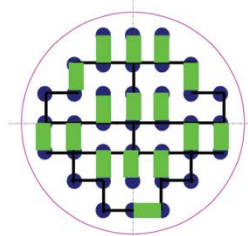
# Experimental work: Rudisuli et al. 2012



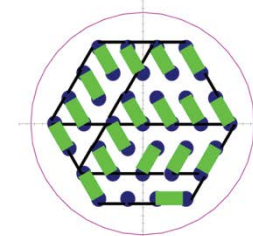
(b) Sq/15/18



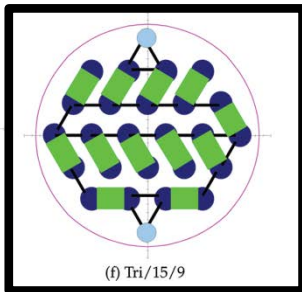
(c) Sq/20/9



(d) Sq/10/9

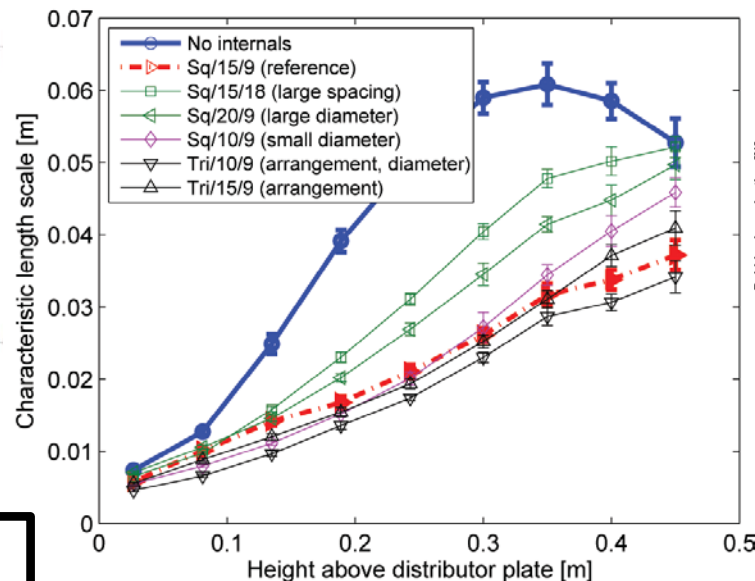


(e) Tri/10/9

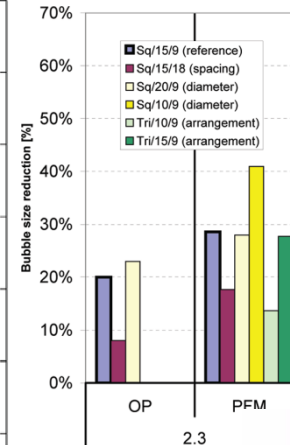


(f) Tri/15/9

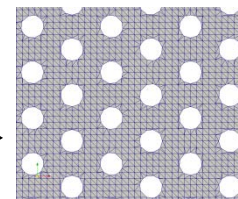
Conf. similar to ADA.inc 1MW pilot plant study



(c)  $u_0/u_{mf} = 6.8$



OP: optical probe measur  
PFM: Pressure fluctuation

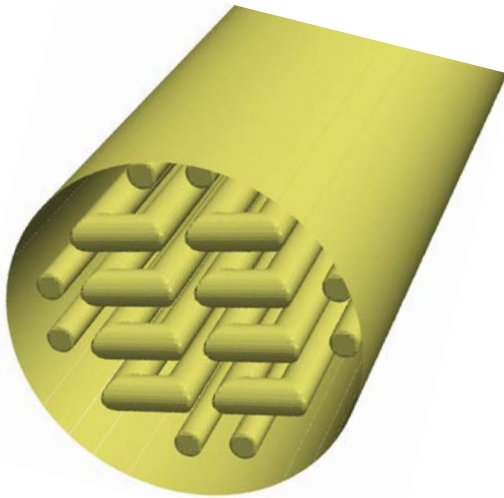


## Fluidized bed configurations

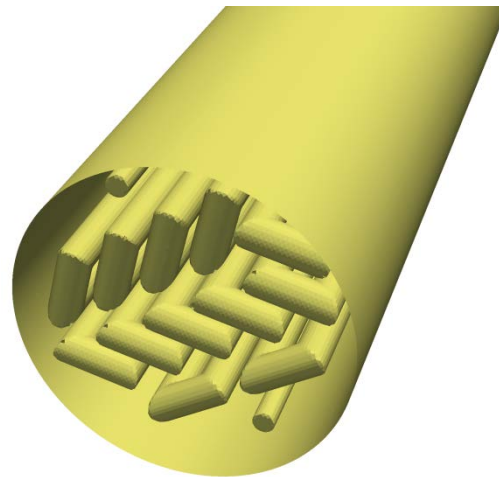
Properties	Without tubes	Sq. arrangement	Tri. arrangement
Column width (number of grids)	0.15 m (100)	0.15 m (100)	0.15 m (100)
Column depth (number of grids)	0.15 m (100)	0.15 m (100)	0.15 m (100)
Column height (number of grids)	0.96 m (640)	0.96 m (640)	0.96 m (640)
Bed diameter from cut-cells	0.145 m	0.145 m	0.145
Number of principal tubes (diameter)	-	16 (15 mm)	24 (15 mm)
Number of auxiliary tubes (diameter)	-	8 (12 mm)	2 (10 mm)

## Particle properties

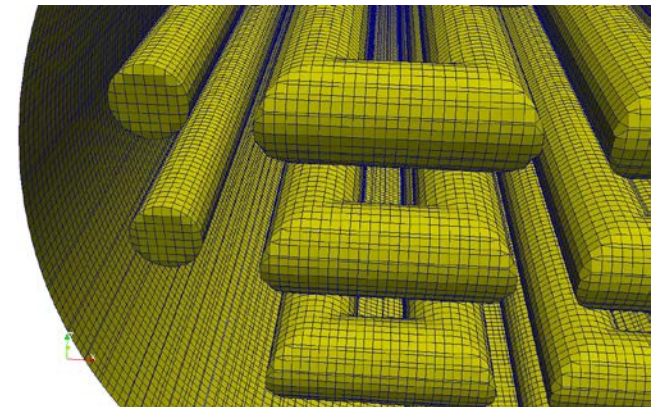
Properties	Values
Particle type	Aluminum oxide
Particle density	1350 kg/m <sup>3</sup>
Particle diameter	289 μm
Coefficient of restitution	0.90
Minimum fluidizing velocity ( $U_{mf}$ )	0.041 m/s
Superficial velocity at inlet ( $U_0$ )	$2.3U_{mf}$ , $4.5U_{mf}$ , $6.8U_{mf}$



Square arrangement



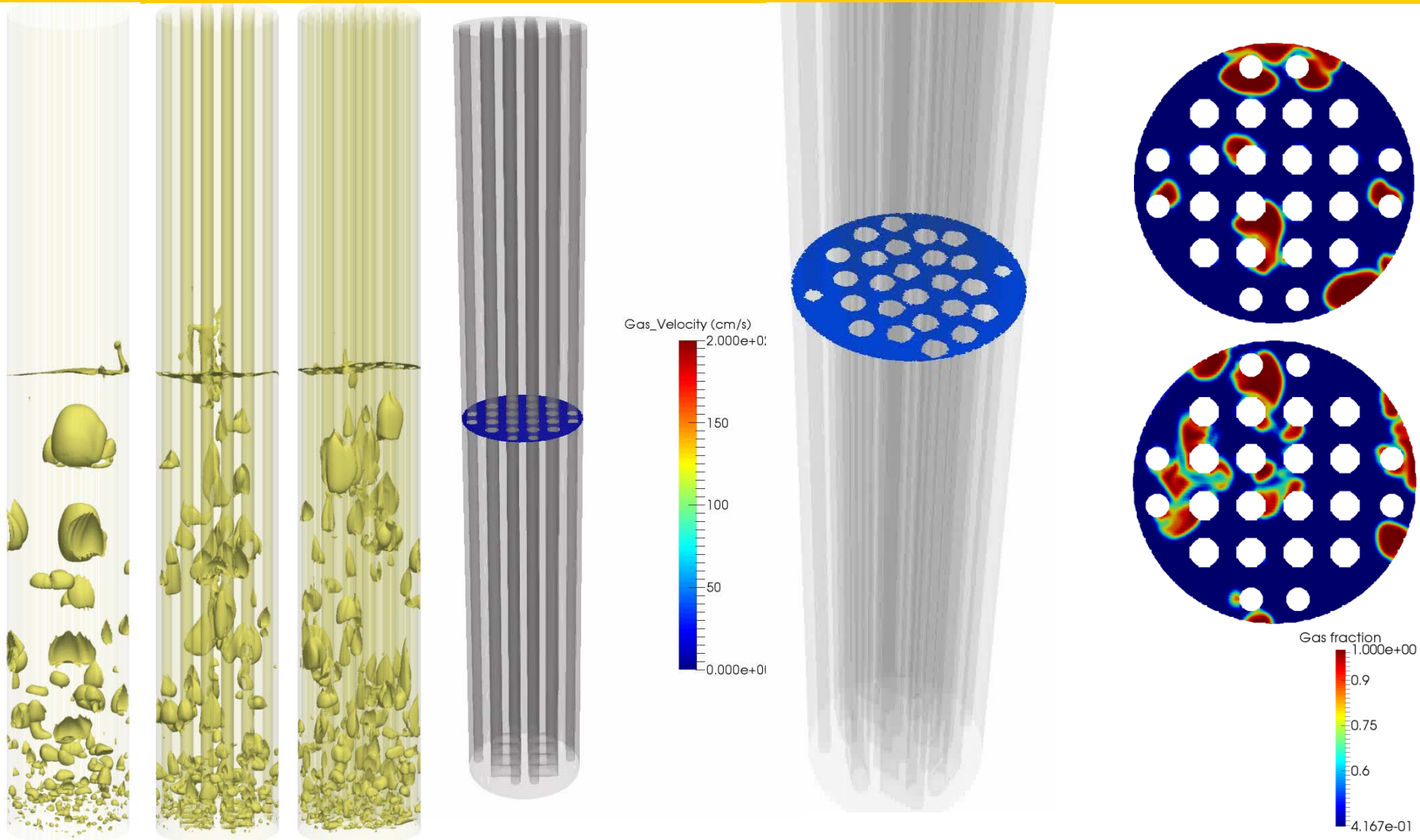
Triangular arrangement



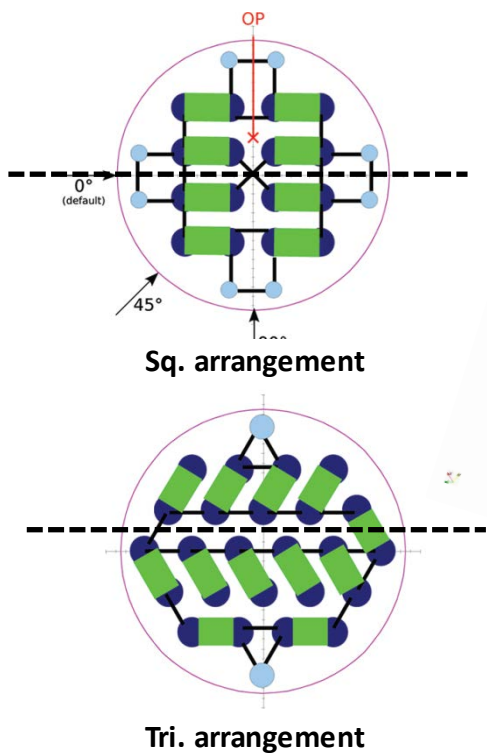
Computational grids

**Computational time:** Real time of 1 s per day using 128 processors on NETL supercomputers for 6.4 million computational cells  
Simulations were performed for 25 s of real time

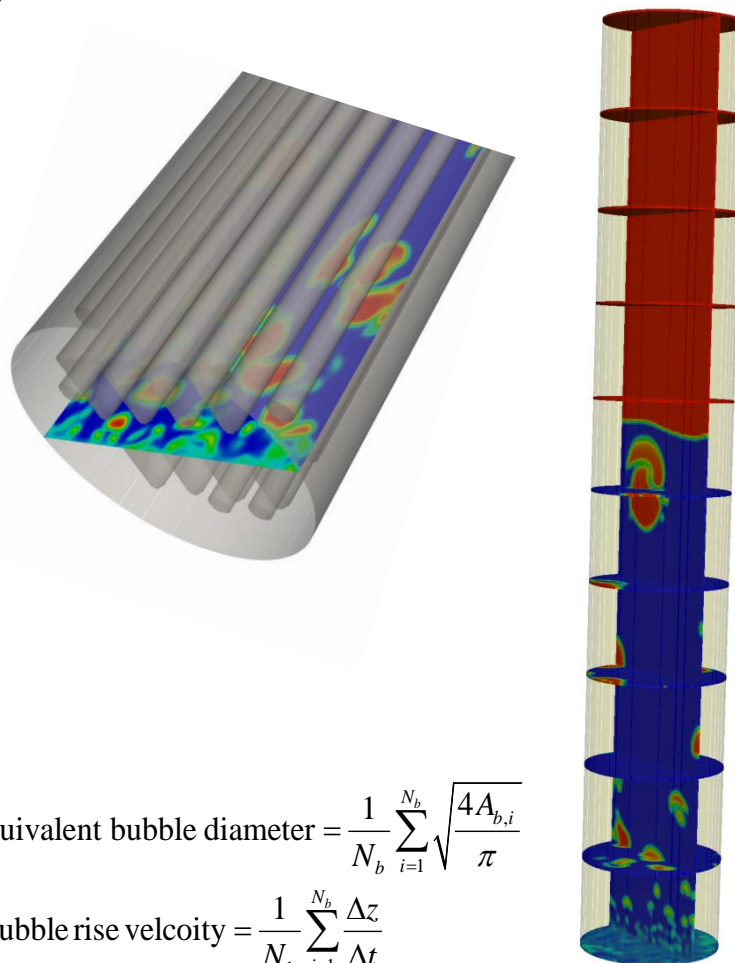
# Snapshots



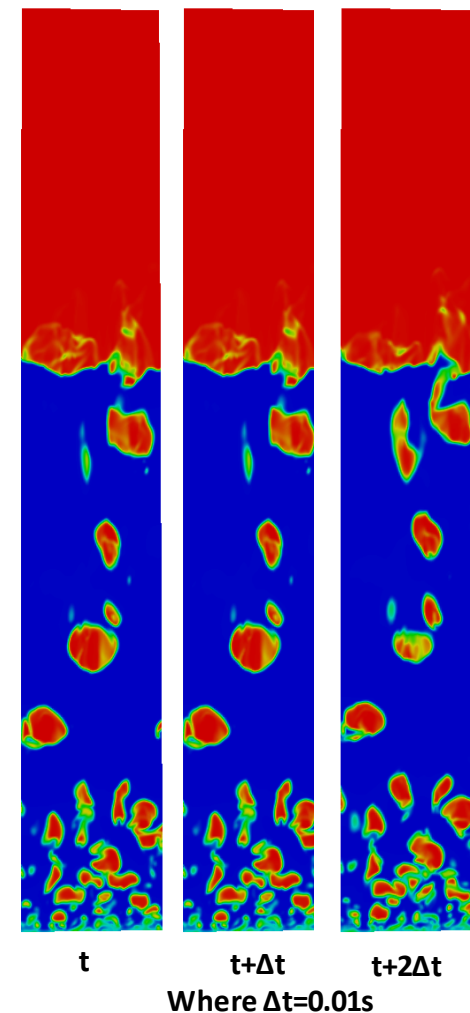
## Plane of measurements



## Data storage 3D domain



## Bubble tracking



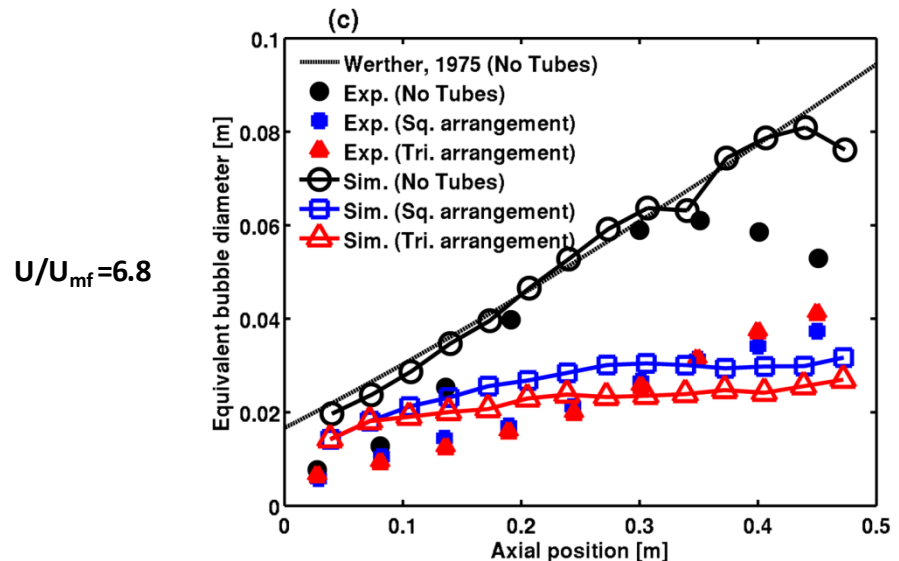
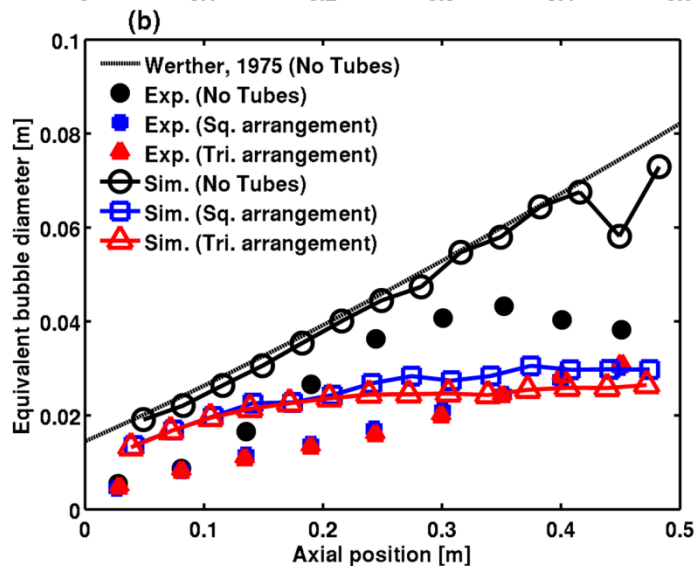
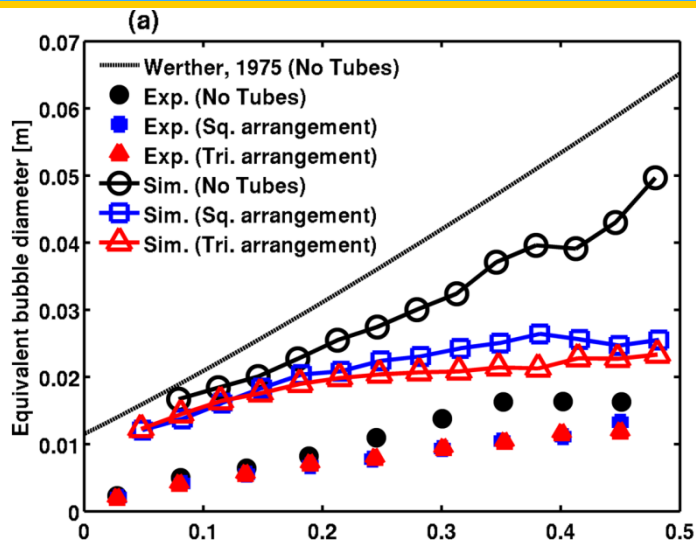
$$\text{Equivalent bubble diameter} = \frac{1}{N_b} \sum_{i=1}^{N_b} \sqrt{\frac{4A_{b,i}}{\pi}}$$

$$\text{Bubble rise velocity} = \frac{1}{N_b} \sum_{i=1}^{N_b} \frac{\Delta z}{\Delta t}$$

$N_b \sim$  Number of bubble detected

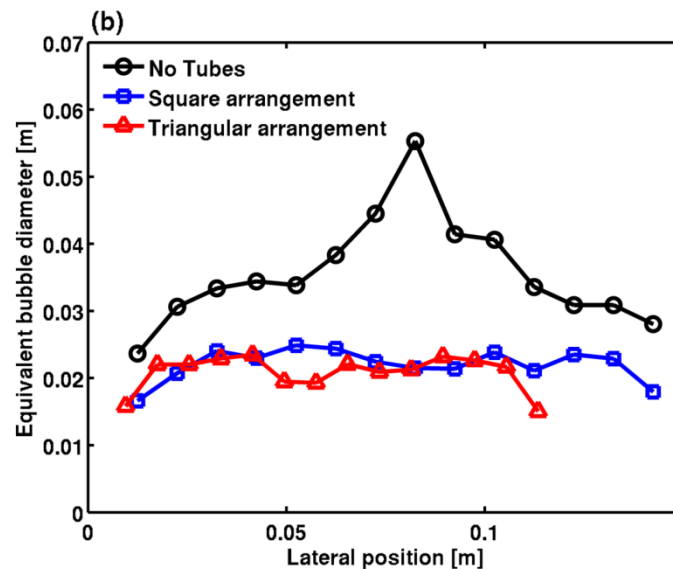
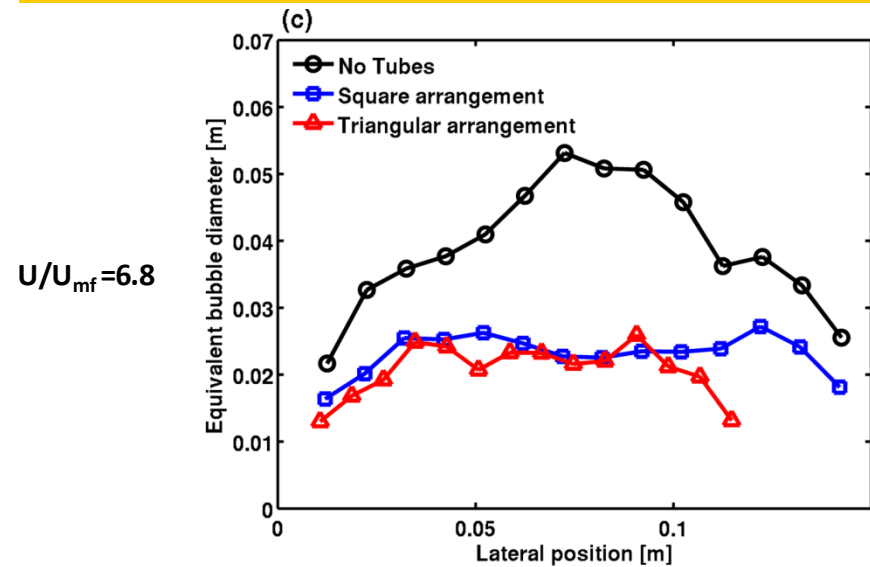
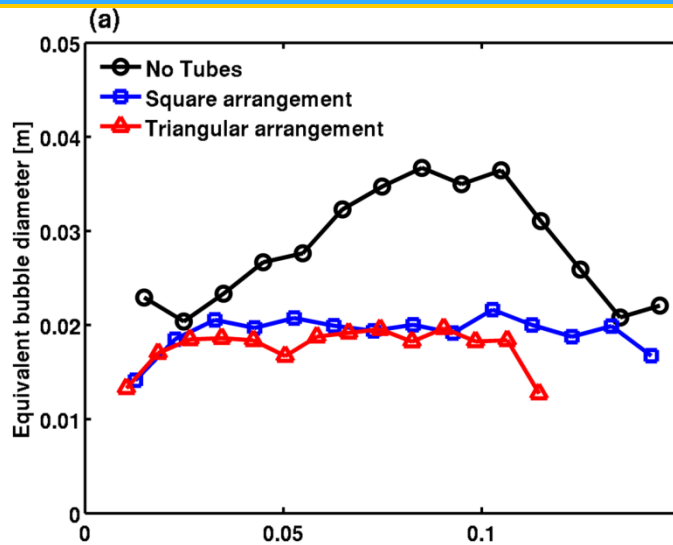
# Simulation Results

# Equivalent bubble diameter



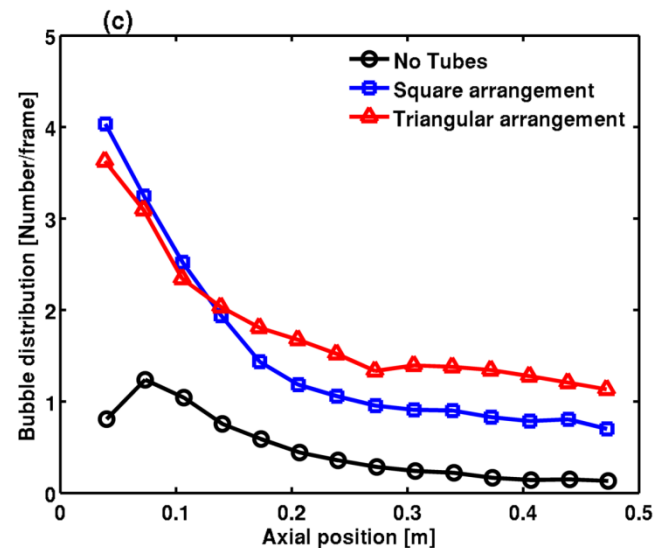
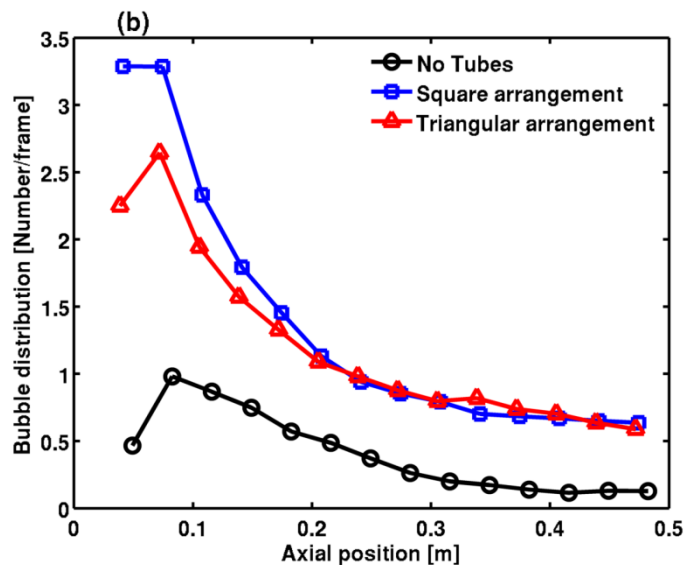
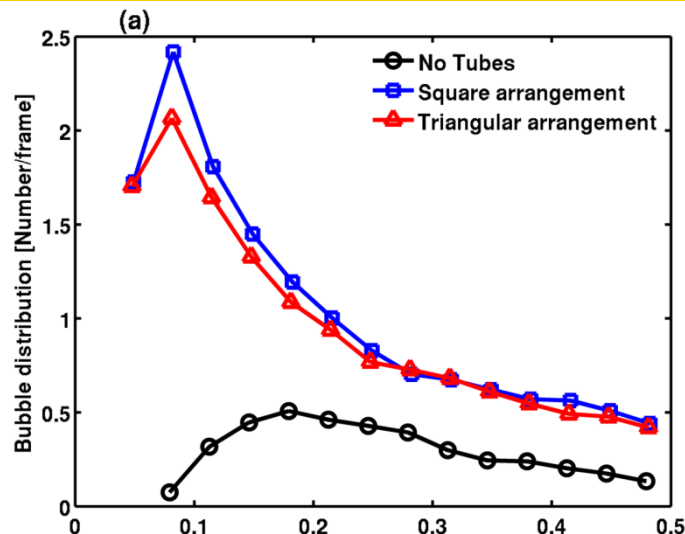
- ✓ Predicted bubble size for no tube is in good agreement with literature correlation of Werther
- ✓ Bubble size decreases with the effect of vertical tubes
- ✓ Sim. and Exp. results are in good agreement for the higher inlet gas velocities of  $U/U_{mf} = 4.8$  and  $6.8$
- ✓ At  $U/U_{mf} = 2.3$  Exp. results are under predicted, considering Sim. result in a close agreement with bubble size correlation of Werther

# Equivalent bubble diameter



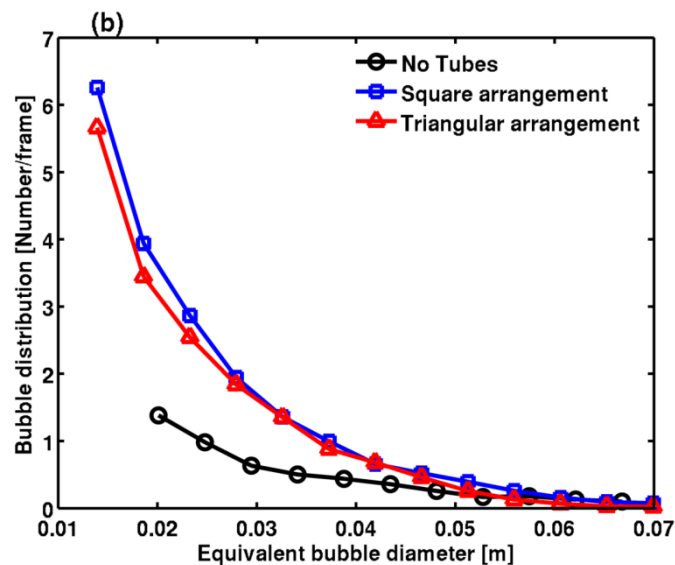
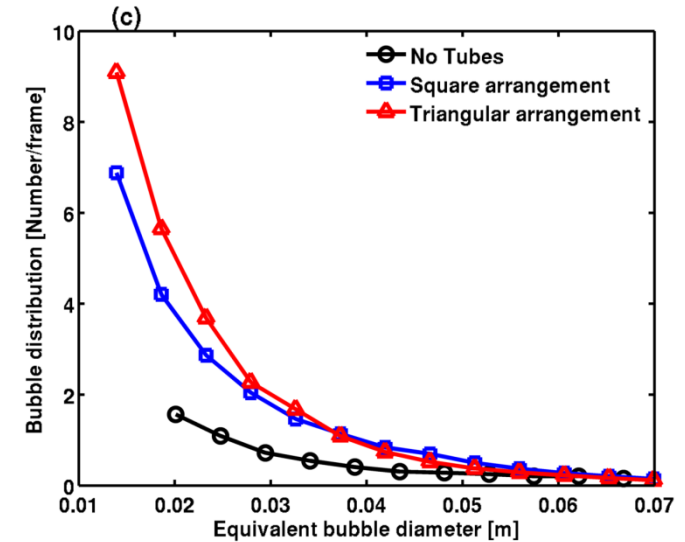
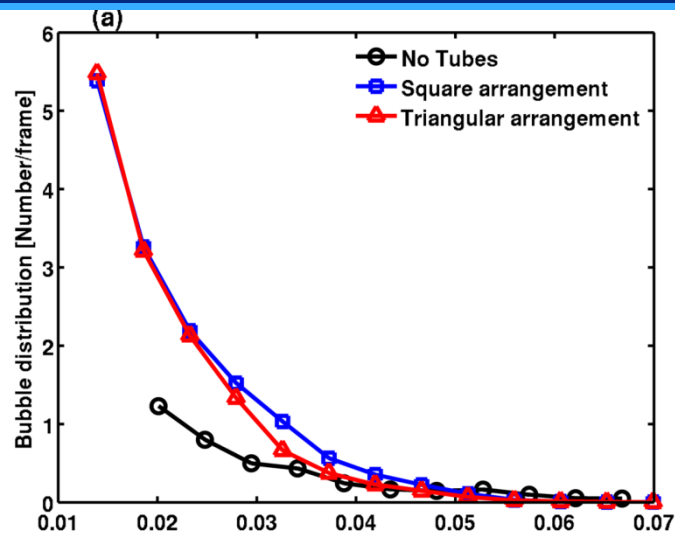
- ✓ Bubble size is larger in the center for No tubes
- ✓ Uniform bubble size predicted across the bed diameter when there are vertical tubes in the bed
- ✓ Vertical tubes prevent coalescence and also promote larger bubbles to split
- ✓ Slugging of bubbles can be prevented using vertical tubes, enhances quality fluidization

# Bubble distribution



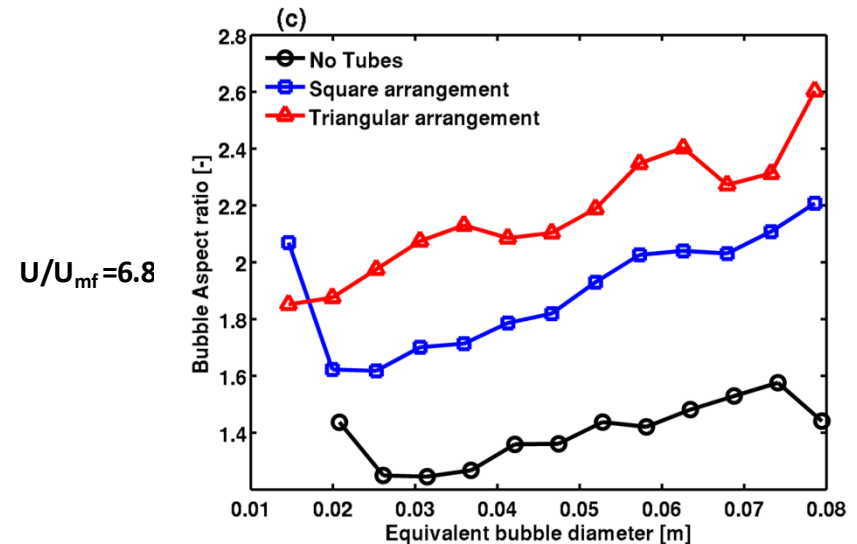
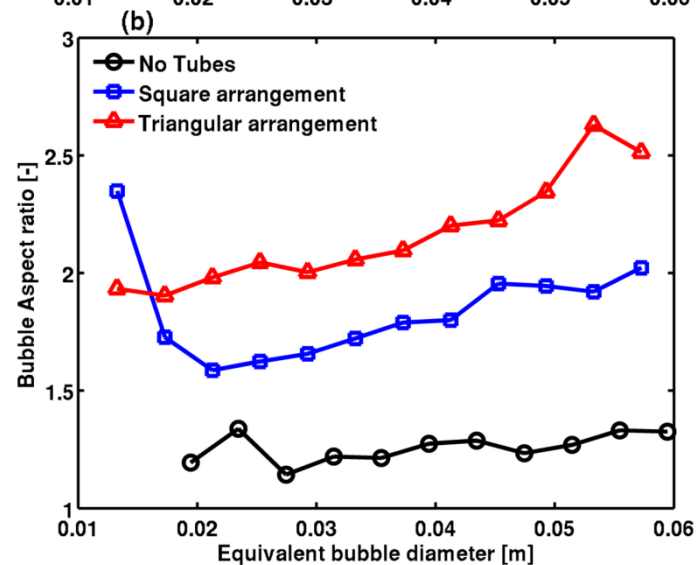
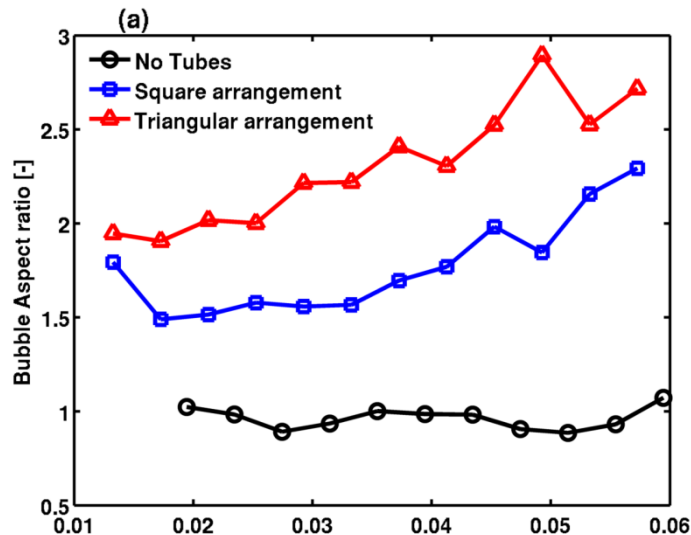
- ✓ For vertical tubes inside, large number of bubbles are predicted throughout the height
- ✓ Significantly more bubbles are predicted in the bottom section of the bed
- ✓ U-shape bank prevents bubble coalescence at the initial stage as the bubble grows
- ✓ Square tube arrangement create parallel chambers for the bubble to rise, hence efficient in preventing bubble coalescence
- ✓ Triangular tube forms staggered alignment of the tubes, promote splitting of larger bubbles

# Bubble distribution



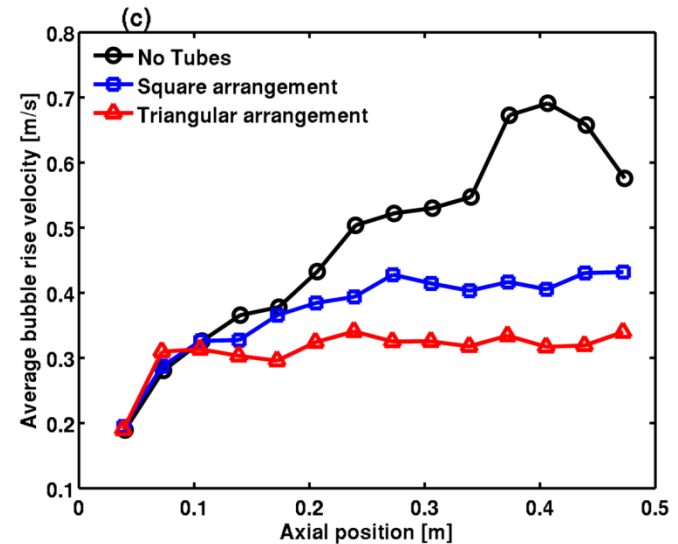
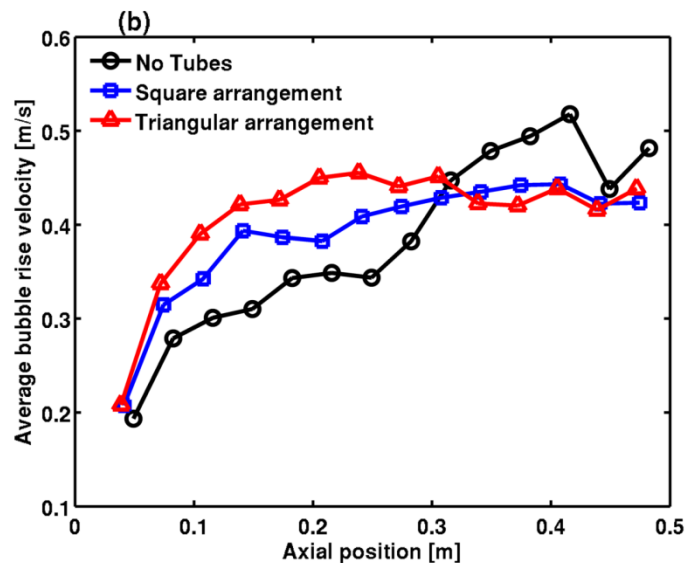
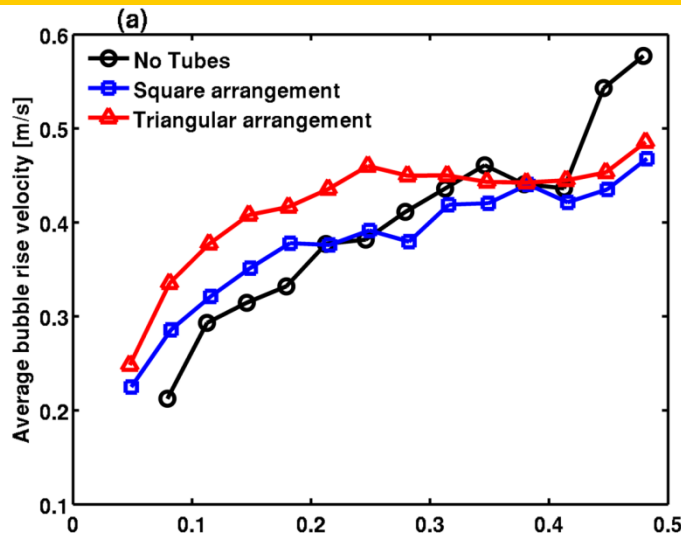
- ✓ Number of small bubbles in the bed is significantly greater for the beds with vertical tubes when compared to the bed with no tubes
- ✓ The number of larger bubbles is similar for both tube arrangements indicating that bubble size is unaffected if it is sufficiently large compared to the tube spacing

# Bubble shape/Aspect ratio



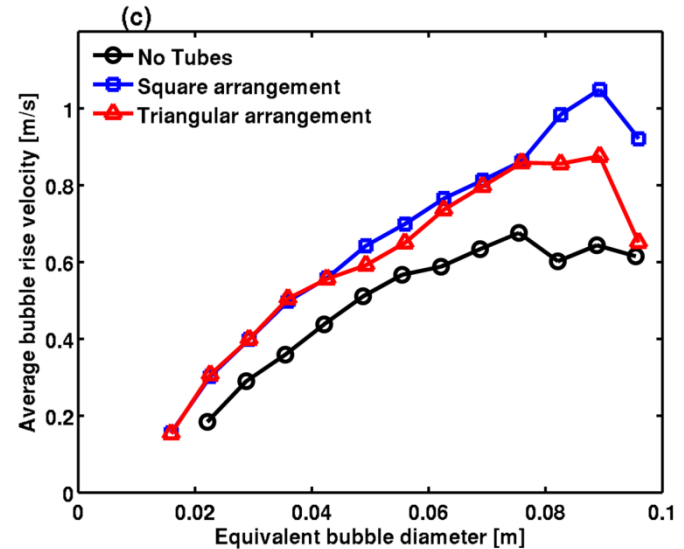
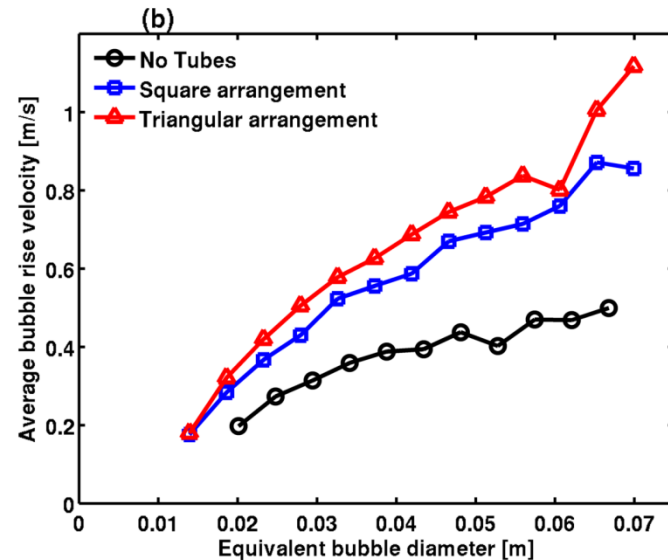
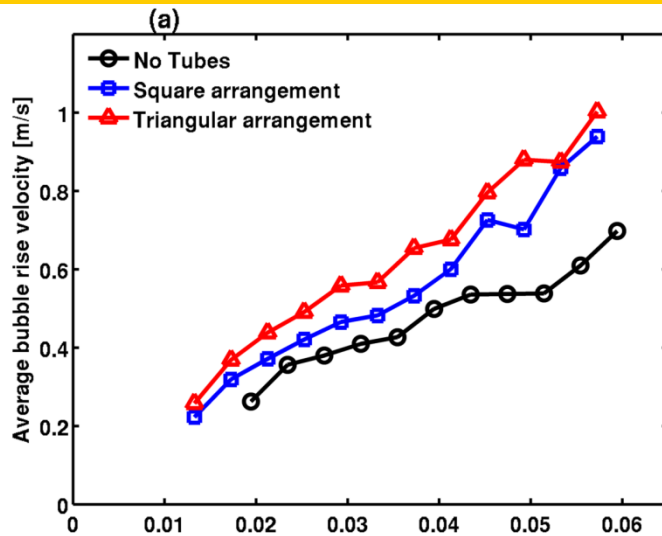
- ✓ The shape of the bubble is estimated from the bubble aspect ratio, i.e. ratio of vertical length to the horizontal length of the bubble
- ✓ For no tubes, bubbles are nearly spherical in shape.
- ✓ Bubbles elongate significantly under the influence of vertical tubes
- ✓ The initial effect of vertical tubes is to squeeze and deform bubbles to fit the space between the tubes
- ✓ Tri. tube arrangements shows considerable difference when compared with Sq. tube arrangement

# Average bubble rise velocity



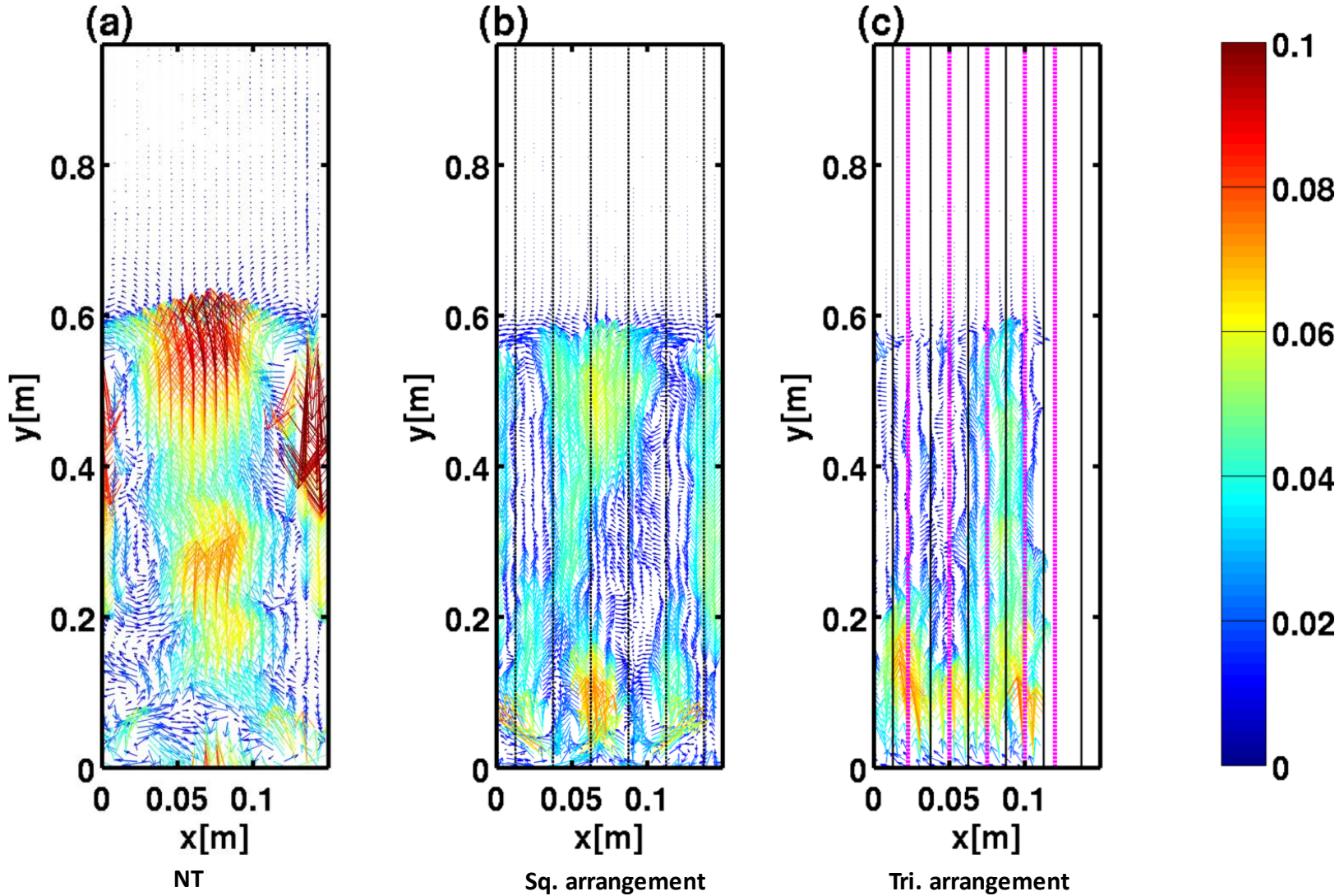
- ✓ Bubble rise velocity shows an increasing trend in the presence of tubes for lower inlet gas velocity
- ✓ At low inlet gas velocities bubble size is comparable to the tube spacing, therefore considerable squeeze occurs between the tubes and bubbles rise faster
- ✓ Squeezing of bubble between the tubes, the centroid of bubble moves a longer distance than uniform size bubble
- ✓ At higher gas velocities, bubble sizes are large enough that they enclose the tube and rise along the tube walls

# Average bubble rise velocity

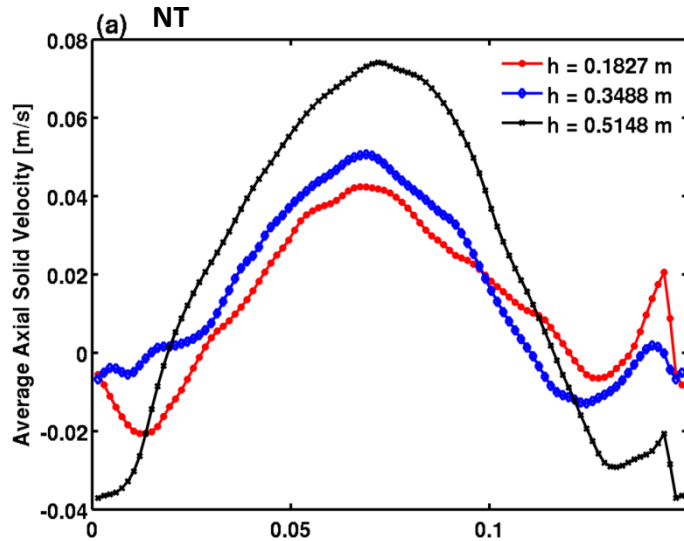


- ✓ Bubbles of the same size rise with different velocities, where bubbles travel faster in the bed with tubes
- ✓ Because the bubble is elongated and follows preferential path along the vertical tubes
- ✓ Bubble rise velocity in the bed with tubes depends upon fluidizing gas velocity and tube arrangements

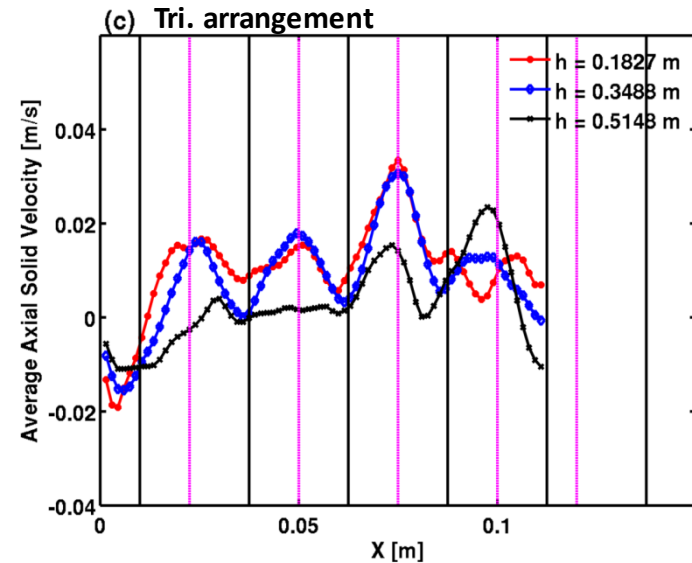
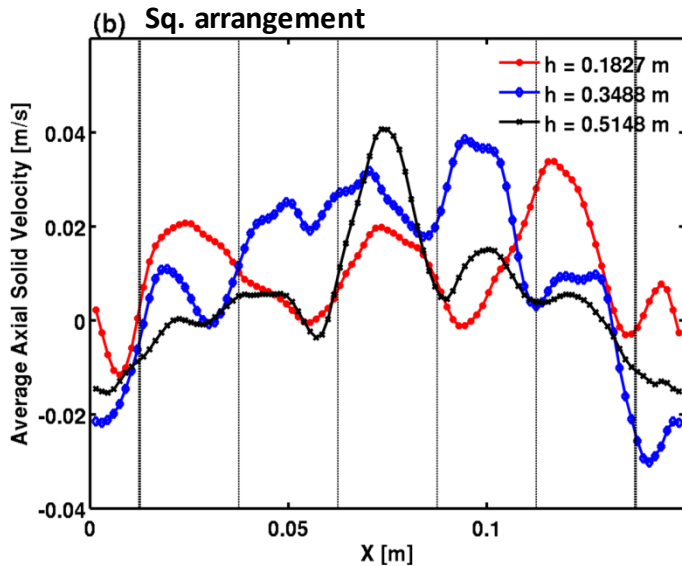
# Solids circulations



# Solids velocity profile

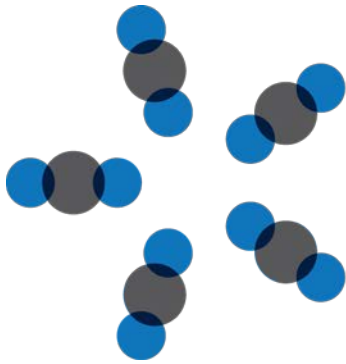


- ✓ Upward motion of solids in the center and downward motion near to the walls for no tubes.
- ✓ For tubes higher solids velocities lie in the region between the tubes.
- ✓ The magnitude of solids velocities is nearly the same at these three heights for vertical tubes.



- ✓ The influence of vertical tubes on bubble characteristics and solids motion in a fluidized bed has been investigated using the MFIX two-fluid model
- ✓ A comparison of simulation results with experimental data shows good agreement
- ✓ Square and triangular tube arrangements have been compared to the bed without tubes
- ✓ A decrease in equivalent bubble diameter and a uniform distribution of bubble are seen for the bed with vertical tubes
- ✓ Simulation results show that the square tube arrangement forms longitudinal, parallel chambers that prevent bubble coalescence
- ✓ Triangular tubes are in a staggered arrangement, they promote bubble splitting
- ✓ Splitting and squeezing of bubbles between the tubes their shapes change significantly, becoming more elongated and travel faster
- ✓ Differences in solids circulation patterns are very distinct for the three bed configurations
- ✓ Solids motion is rarely seen in the radial direction because the vertical tubes prevent lateral solids motion

# Acknowledgements



# CCSI

Carbon Capture Simulation Initiative

This work is performed in support of the U.S. Department of Energy, Office of Fossil Energy's Carbon Capture Simulation Initiative (CCSI)

**Thank you**

**Questions ?**

## **Disclaimer**

This presentation was prepared as an account of work sponsored by an agency of the United States Government. Neither the United States Government nor any agency thereof, nor any of their employees, makes any warranty, express or implied, or assumes any legal liability or responsibility for the accuracy, completeness, or usefulness of any information, apparatus, product, or process disclosed, or represents that its use would not infringe privately owned rights. Reference herein to any specific commercial product, process, or service by trade name, trademark, manufacturer, or otherwise does not necessarily constitute or imply its endorsement, recommendation, or favoring by the United States Government or any agency thereof. The views and opinions of authors expressed herein do not necessarily state or reflect those of the United States Government or any agency thereof.